Online Supplemental Methods and Data

Transplantation of Bone Marrow Cells from miR150 Knockout Mice Improves Senescence-associated Humoral Immune Dysfunction and Arterial Stiffness

Jun Fan, Shirley Wang, Xianglan Lu and Zhongjie Sun

Department of Physiology, College of Medicine, University of Tennessee Health Science Center, Memphis, TN 38163, USA
Department of Physiology, College of Medicine, University of Oklahoma Health Science Center, Oklahoma City, OK 73034, USA

Running title: BMT and arterial stiffness and hypertension in SAMP1 mice

Address Correspondence to:

Zhongjie Sun, MD, PhD, FAHA
Professor and Chair
Department of Physiology
College of Medicine
University of Tennessee Health Sciences Center
A302 Coleman Building
956 Court Avenue
Memphis, TN 38163
USA
Zsun10@uthsc.edu
Tel. 901-448-2679

Disclosures: Nothing to disclose

Current address of Jun Fan, Department of Tissue Engineering, School of Intelligent Medicine, China Medical University, Shenyang, 110122, China.

Online Supplemental Methods

Bone marrow transplantation

The intra-bone marrow-bone marrow transplantation (IBM-BMT) was carried out according to the method reported previously [1]. SAMP1 mice (female, 10 month old) received bone marrow cells (BMCs) from age-matched of male miR-150 KO mice (SAMP1+miR-150 KO-BMC) and male C57BL/6 mice (SAMP1+WT-BMC) respectively. The tibia and femur bones were extracted from miR-150 KO mice and C57BL/6 mice, and bone marrow was obtained as described previously [2]. The whole BMCs were directly injected into the bone marrow cavity (IBM-BMT) of the tibia of SAMP1 mice. In brief, the knee was flexed to 90 degrees and the proximal side of the tibia was drawn to the anterior (Fig. S1). A 26-gauge needle was inserted into the joint surface of the tibia through the patellar tendon and then inserted into the bone marrow cavity. The donor BMCs (1×10^7) were injected into the bone marrow cavity using a microsyringe (30 μl; Hamilton Co., Reno, NV).

Measurement of Pulse Wave Velocity

Aortic PWV was assessed as we described previously [3-5]. Briefly, mice were anesthetized under 2% isoflurane in a closed chamber anesthesia machine (SomnoSuite, Kent Scientific, Torrington, CT) for ~1–3 min. Anesthesia was maintained via a nose cone, and mice were placed supine on a heating board (~37°C) with legs secured to ECG electrodes. Velocities were measured with 6-mm crystal 20-MHz Doppler probes (Indus Instruments, Webster, TX) at the transverse aortic arch and at the abdominal aorta and collected using Doppler signal processing workstation (Indus Instruments). Absolute pulse arrival times were indicated by the sharp upstroke, or foot, of each velocity waveform. Aortic PWV was calculated by the thoracic-abdominal distance divided by the pulse transit time between flow pulses recorded at the thoracic and abdominal aortic sites.

Measurements of Blood Pressure

BP was measured as described previously [5-10]. Briefly, blood pressure (BP) was measured by the volume-pressure recording (VPR) tail-cuff method using a CODA BP monitoring system (Kent Scientific) as described previously [5-9]. This none-invasive method involves slight

warming (28°C) but not heating of the tail. Briefly, the animals were gently handled and well trained daily for the VPR tail-cuff measurement to minimize the handling stress. No signs of stress were observed during BP measurements. The VPR tail-cuff procedure can reliably monitor BP and is a common method for monitoring BP in our laboratory. This method has been validated by using a telemetry system [11]. The operator was also strictly trained for the measurement procedure. At least 20 stable cycle data were obtained from each mouse for the result analysis. We confirmed in our previous studies that this method is a reliable procedure for monitoring blood pressure [5, 8, 10].

Histological staining

Briefly, thoracic aortas were quickly excised and placed in cold (4°C) physiological salt solution. The aortic rings (5 mm) with perivascular tissue intact were removed from the thoracic aorta directly distal to the greater curvature of the aortic arch. Aorta tissue was post-fixed in 4% paraformaldehyde, embedded in paraffin and sectioned at 5 μm thickness. Five sections of each mouse (6 mice per group) were processed for staining. Collagen staining was assessed by mason's trichrome stain as described previously [6, 7, 12-14]. The blue staining represented collagen deposition. Elastin was stained by Vehoeff's elastic stain kit (American MasterTech). The black staining represented elastin in the aorta. The semi-quantitative analysis of relative collagen and elastin area fraction (percentage of blue-stained collagen area over the total area in one field) was measured using NIS-Elements BR 3.0 software.

Immunohistochemistry

Briefly, a series of 5-μm-thick sections of paraffin-embedded aortas were cut and deparaffinized, rinsed in xylene, and rehydrated. CD3 (ab5690, Abcam) and CD68 (ab31630, Abcam) were used for analysis. Diluted primary antibodies were then applied to the sections, and these sections were incubated overnight at 4°C and then with appropriated secondary antibodies conjugated with HRP at room temperature for 60 minutes. Stable diaminobenzidine (DAB, Invitrogen) was used as a substrate for peroxidase. Slides were counterstained with hematoxylin. All sections were then dehydrated in graded alcohols and covered by coverslips with neutral balsam for light microscopy. For negative control experiments, the primary antibody was omitted and processed

as described earlier [5, 15]. Non-specific staining was not observed. Images of aortas from consecutive cross sections for each animal were collected at equal exposure conditions and at the same magnification (40X objective lens). The number of cells with positive CD3 or CD68-staining in the aorta was counted in NIS-Elements BR 3.0 (Nikon).

Western Blot Analysis

Protein samples from the thoracic aorta were prepared in lysis buffer for western blot analysis as described previously [15-17]. Briefly, the proteins (15µg) were separated by SDS-PAGE and transferred onto nitrocellulose membrane (Bio-Rad). The membrane was then incubated overnight (4°C) with a primary antibody against Collagen I (1:1000, ab765p, Abcam), elastin (1:1000, ab217356, Abcam), MMP-2 (1:1000, AB19015, Millipore,), MMP-9 (1:1000, AB19016,Millipore), TGFβ-1 (1:100, sc-130348, Santa Cruz Biotechnology), Scleraxis (1:100, sc-518082, Santa Cruz Biotechnology), MCP-1 (1:1000, 2029, Cell Signaling), TNF-α (1:1000, 119485, Cell Signaling), VCAM-1 (1:200, sc-8304, Santa Cruz Biotechnology), ICAM-1 (1:200, sc-8439, Santa Cruz Biotechnology), IL-6 (1:1000, ab208113, Abcam), and β-actin (1:10000, ab8226, Abcam). Goat anti-mouse or goat anti-rabbit conjugated with horseradish peroxidase (1:3000–1:5,000; Santa Cruz Biotechnology) was used as a secondary antibody and incubated for 1 hour at room temperature. Specific proteins were detected by chemiluminescent methods using Amersham™ ECL™ western blotting detection reagents (GE Healthcare, UK). Protein abundance on western blots was captured using Chem-Doc (Bio-Rad) and quantified by densitometry using Image lab software (Bio-Rad, Hercules, CA).

Measurement of serum IgG and IgM ELISA

Mouse serum IgG and IgM concentrations were measured using commercial ELISA kits (Bethyl Laboratories Incorporated, Montgomery, TX, USA) according to manufacturer's instructions.

Flow cytometry

At the end of the treatment, the blood and bone marrow were collected. Total blood was drawn *via* heart puncture in euthanized mice and diluted with one volume of PBS. The bone marrow cells collected from the tibia and femur were also diluted with PBS and filtered. Load the cell

suspension onto Ficoll. After the gradient separation, mononuclear cells were collected. Cells were stained with fluorescent marker-conjugated antibodies and analyzed using a FACS CantoII instrument (BD Biosciences). APC-conjugated anti-CD19 (1:200, B cell epitopes) and PE-conjugated anti-CD3 (1:200, T cell epitopes) were used. All antibodies were purchased from BD Biosciences, Data were obtained using BD FACSCanto II or FACSAria II and analyzed using Flow Jo software (Tree Star, Ashland, OR, USA).

Cell Culture

Human Umbilical Vein Endothelial Cells (HUVECs) (Lonza, Basel, Switzerland) were cultured in EBM-2 medium (Lonza) using a Bulletkit (Lonza) containing growth factors and incubated at 37 °C in a 5% CO_2 incubator. Cells at the third passage were used in all experiments. After 80–90% confluence was obtained, the medium was refreshed and cells were cultured in DMEM with 10% normal FBS (Thermo Fisher Scientific) or 10% Ultra-Low IgG FBS (Thermo Fisher Scientific) with or without 0.2mg/ml IgG from bovine serum (bIgG, Sigma) for 24h before cells were collected for Western blot analysis.

References

[1] Kushida T, Inaba M, Hisha H, Ichioka N, Esumi T, Ogawa R, et al. Intra-bone marrow injection of allogeneic bone marrow cells: a powerful new strategy for treatment of intractable autoimmune diseases in MRL/lpr mice. Blood. 2001;97:3292-9.

[2] Kanamaru T, Kamimura N, Yokota T, Nishimaki K, Iuchi K, Lee H, et al. Intravenous transplantation of bone marrow-derived mononuclear cells prevents memory impairment in transgenic mouse models of Alzheimer's disease. Brain research. 2015;1605:49-58.

[3] Hartley CJ, Taffet GE, Michael LH, Pham TT, Entman ML. Noninvasive determination of pulse-wave velocity in mice. The American journal of physiology. 1997;273:H494-500.

[4] Reddy AK, Li YH, Pham TT, Ochoa LN, Trevino MT, Hartley CJ, et al. Measurement of aortic input impedance in mice: effects of age on aortic stiffness. Am J Physiol Heart Circ Physiol. 2003;285:H1464-70.

[5] Feng R, Ullah M, Chen K, Ali Q, Lin Y, Sun Z. Stem cell-derived extracellular vesicles mitigate ageing-associated arterial stiffness and hypertension. Journal of extracellular vesicles. 2020;9:1783869.

[6] Chen K, Sun Z. Activation of DNA demethylases attenuates aging-associated arterial stiffening and hypertension. Aging Cell. 2018:e12762.

[7] Chen K, Zhou X, Sun Z. Haplodeficiency of Klotho Gene Causes Arterial Stiffening via Upregulation of Scleraxis Expression and Induction of Autophagy. Hypertension. 2015;66:1006-13.

[8] Lin Y, Chen J, Sun Z. Antiaging Gene Klotho Deficiency Promoted High-Fat Diet-Induced Arterial Stiffening via Inactivation of AMP-Activated Protein Kinase. Hypertension. 2016;67:564-73.

[9] Zhou X, Chen K, Lei H, Sun Z. Klotho gene deficiency causes salt-sensitive hypertension via monocyte chemotactic protein-1/CC chemokine receptor 2-mediated inflammation. J Am Soc Nephrol. 2015;26:121-32.
[10] Gao D, Zuo Z, Tian J, Ali Q, Lin Y, Lei H, et al. Activation of SIRT1 Attenuates Klotho Deficiency-Induced Arterial Stiffness and Hypertension by Enhancing AMP-Activated Protein Kinase Activity. Hypertension. 2016;68:1191-9.
[11] Whitesall SE, Hoff JB, Vollmer AP, D'Alecy LG. Comparison of simultaneous measurement of mouse systolic arterial blood pressure by radiotelemetry and tail-cuff methods. American journal of physiology Heart and circulatory physiology. 2004;286:H2408-15.
[12] Zhou X, Chen K, Lei H, Sun Z. Klotho Gene Deficiency Causes Salt-Sensitive Hypertension via Monocyte Chemotactic Protein-1/CC Chemokine Receptor 2-Mediated Inflammation. Journal of the American Society of Nephrology : JASN. 2014.
[13] Chen J, Lin Y, Sun Z. Deficiency in the anti-aging gene Klotho promotes aortic valve fibrosis through AMPKalpha-mediated activation of RUNX2. Aging Cell. 2016;15:853-60.
[14] Chen J, Fan J, Wang S, Sun Z. Secreted Klotho Attenuates Inflammation-Associated Aortic Valve Fibrosis in Senescence-Accelerated Mice P1. Hypertension. 2018;71:877-85.
[15] Gao D, Wang S, Lin Y, Sun Z. In vivo AAV delivery of glutathione reductase gene attenuates anti-aging gene klotho deficiency-induced kidney damage. Redox Biol. 2020;37:101692.
[16] Chen K, Kobayashi S, Xu X, Viollet B, Liang Q. AMP activated protein kinase is indispensable for myocardial adaptation to caloric restriction in mice. PloS one. 2013;8:e59682.
[17] Chen K, Sun Z. Autophagy plays a critical role in Klotho gene deficiency-induced arterial stiffening and hypertension. J Mol Med (Berl). 2019;97:1615-25.

Online Supplemental Data

A

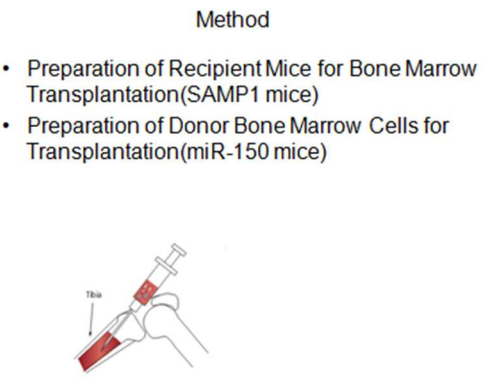

B

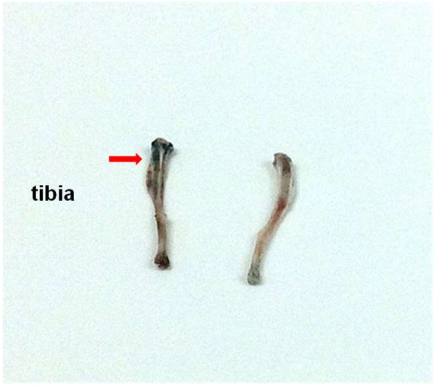

Supplemental Figure S1. (**A),** Preparation of receipt and donor mice for bone marrow transplantation. (**B),** Bone marrow cells (BMCs) from C57 mice and miR-150 KO mice were injected directly into the bone marrow cavity of the tibia of SAMP1 mice under anesthesia. The red arrow indicates that trypan blue in the bone marrow cavity of the tibia.

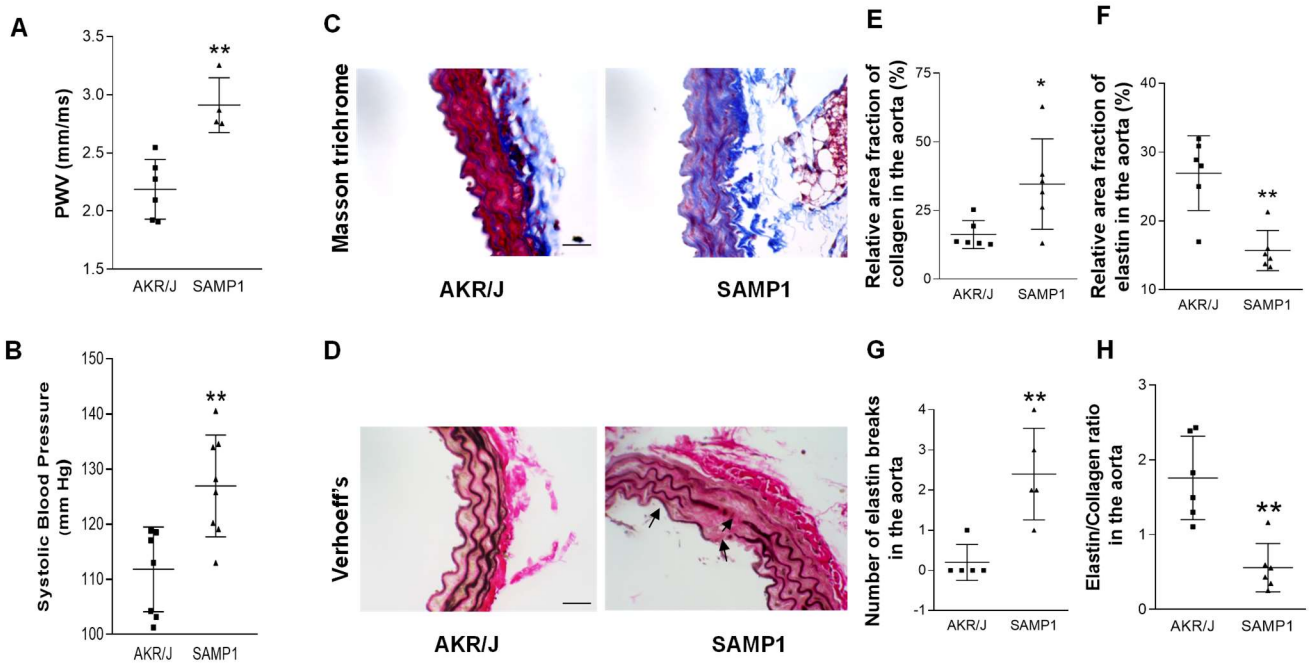

Supplemental Figure S2. SAMP1 mice developed arterial stiffness and hypertension (10 months). **(A)** Pulse wave velocity (PWV). **(B)** Systolic blood pressure. **(C)** Representative Masson-stained sections showing collagen expressionin the aorta. The blue stainning indicates collagen. **(D)** Representative Verhoeff's staining showing elastin expression. The dark staining indicates the elastin lamella. Arrows point to the elastin lamella breaks in the aorta sections. **(E)** Semiquantitative analysis of collagen levels in the aorta. **(F)** Semiquantitative analysis of elastin levels in the aorta. **(G)** The number of elastin lamella breaks in the aorta sections. **(H)** The ratio of elastin/collagen in the aorta. Scale bar indicates 100 μm. Data = mean ± SEM (n=4-8). Student's t-test was performed. *P<0.05, **P<0.01 *Vs* AKR/J mice.

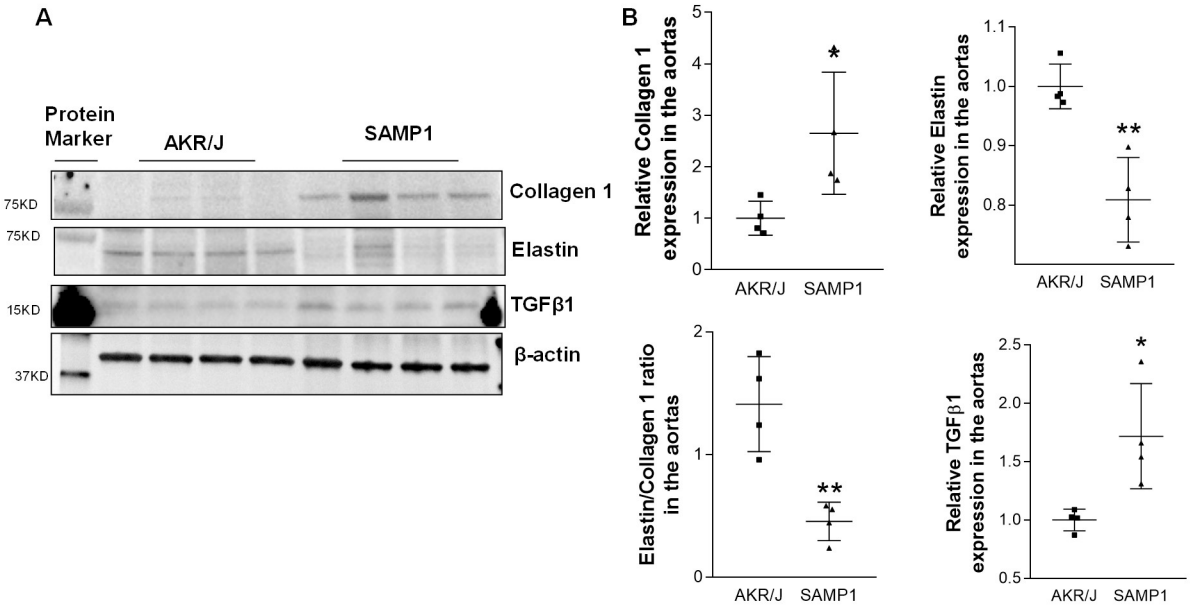

Supplemental Figure S3. Aortic expression of collagen 1, elastin and TGFβ1 in SAMP1 mice. (A) Representative Western blot bands of collagen I, elastin and TGFβ1. **(B)** Quantitative analysis of collagen1, elastin and TGFβ1. Protein expression of collagen 1, elastin and TGFβ1 was first normalized with β-actin and then calculated as fold changes *vs.* the AKR/J group. Data = mean ± SEM (n=4). Student's *t*-test was performed. *P<0.05, **P<0.01 *Vs* AKR/J mice.

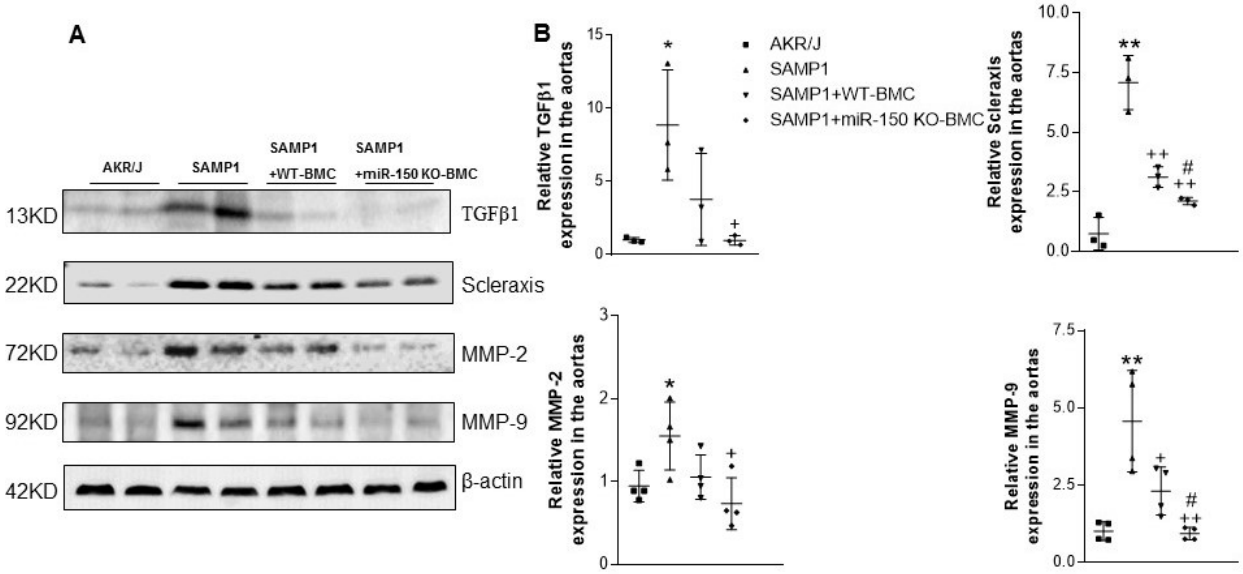

Supplemental Figure S4. Transplantation of BMCs from miR-150 KO mice attenuated expression of TGF-β1, Scleraxis, MMP-2 and MMP-9 in aortas of SAMP1 mice. The analysis was performed at 8 weeks after the BMT. **(A)** Representative Western blot bands of TGFβ1, Scleraxis, MMP-2 and MMP-9. **(B)** Quantitative analysis of TGFβ1, Scleraxis, MMP-2, and MMP-9. The target bands were first normalized with β-actin and then calculated as fold changes *vs.* the AKR/J group. Data = mean ± SEM (n=3-4). One-way ANOVA analysis with Bonferroni correction was performed. *P<0.05, ** P<0.01 *Vs* AKR/J mice; $^{+}$P<0.05, $^{++}$P<0.01 *Vs* SAMP1 mice; $^{\#}$P<0.05 *Vs* SAMP1+WT-BMC mice.

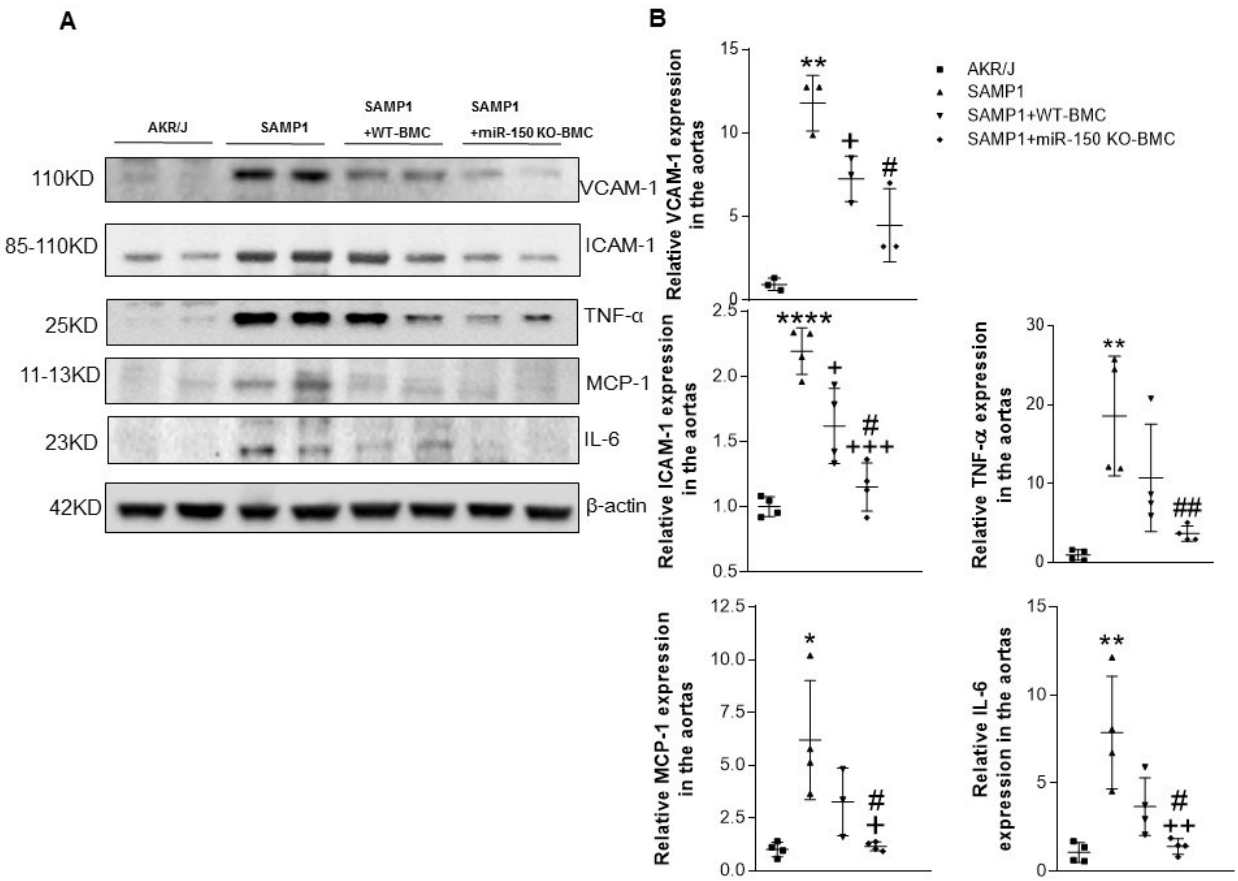

Supplemental Figure S5. Transplantation of BMCs from miR-150 KO mice effectively mitigated vascular inflammatory activation in SAMP1 mice. The analysis was performed at 8 weeks after the BMT. **(A)** Representative Western blot bands of VCAM-1, ICAM-1, MCP-1, TNF-α and IL-6. **(B)** Quantitative analysis of VCAM-1, ICAM-1, MCP-1, TNF-αand IL-6. The target bands were first normalized with β-actin and then calculated as fold changes *vs.* the AKR/J group. Data = mean ± SEM (n=3-4). One-way ANOVA analysis with Bonferroni correction was performed. *P<0.05, ** P<0.01 *Vs* AKR/J mice; $^{+}$P<0.05 *Vs* SAMP1 mice; $^{\#}$P<0.05, $^{\#\#}$P<0.01 *Vs* SAMP1+WT-BMC mice.

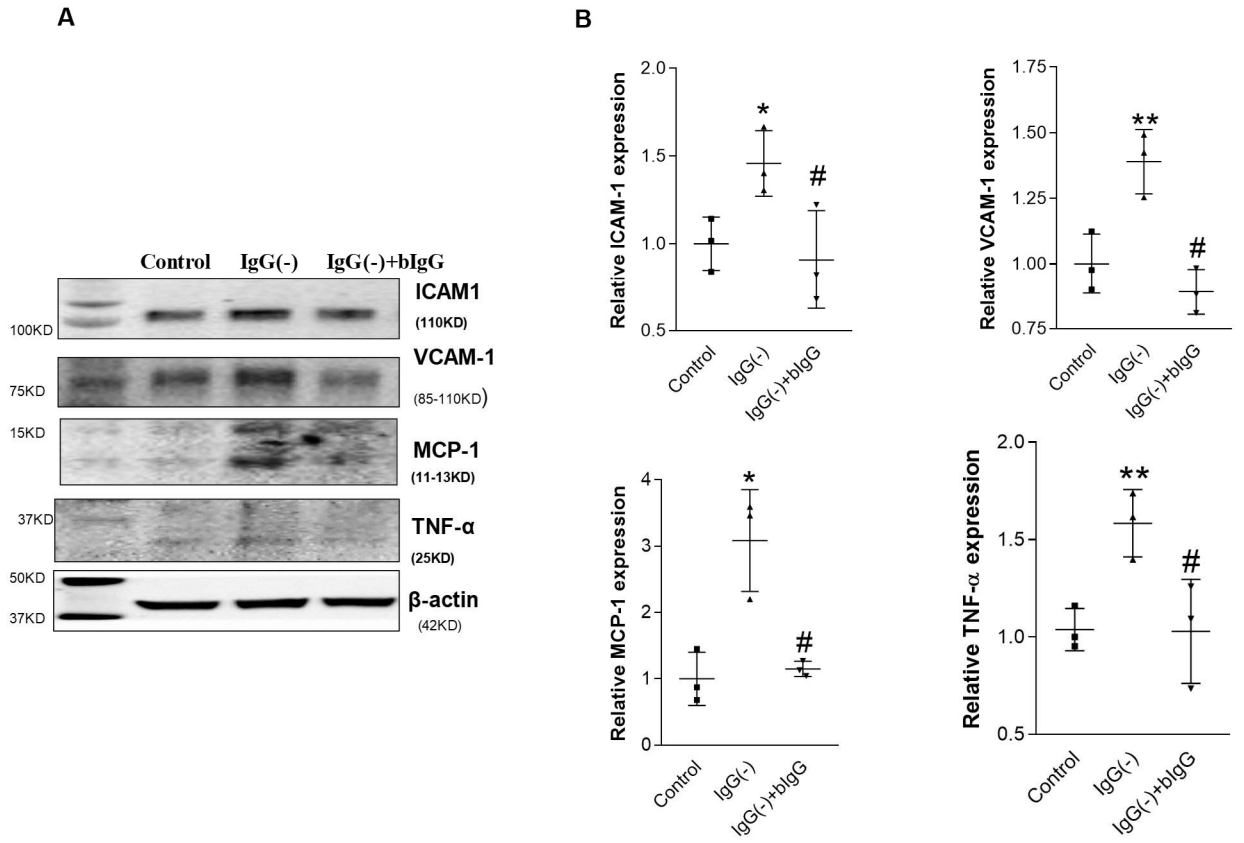

Supplemental Figure S6. IgG protein attenuated the IgG deficiency-induced increases in inflammatory factor expression in vascular endothelial cells. **(A)** Representative Western blot bands of ICAM-1, VCAM-1, MCP-1and TNF-α. **(B)** Quantification of ICAM-1, VCAM-1, MCP-1 and TNF-α expression. The data were first normalized with β-actin and then calculated as fold changes of the control group. Data = mean ± SEM. n=3 independent experiments. One-way ANOVA analysis with Bonferroni correction was performed. *p< 0.05, **p<0.01 *vs.* the control group; $^{\#}$p<0.05 *vs.* the IgG-deficient-serum group.

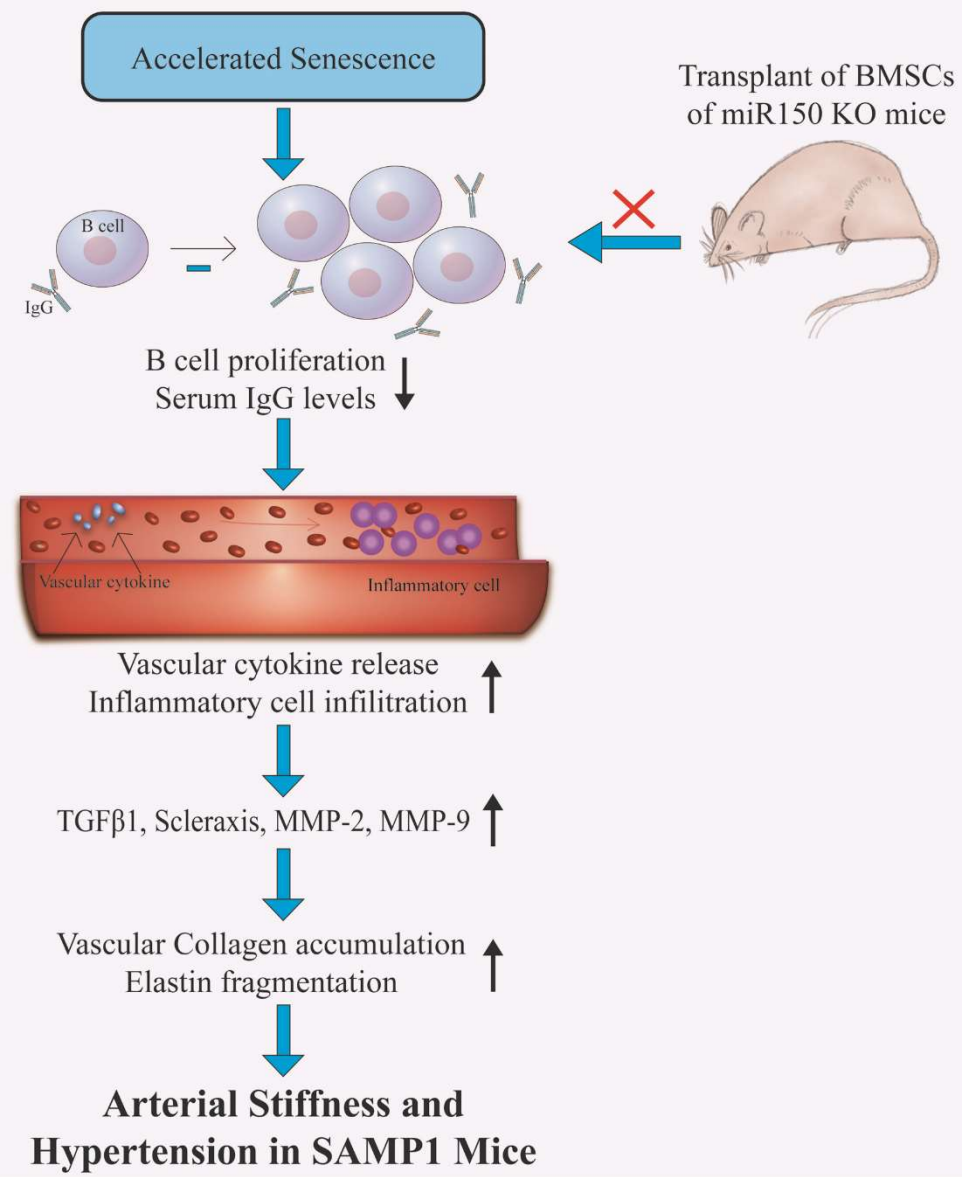

Supplemental Figure S7. The mechanistic pathway that mediates the beneficial effect of BMC transplantation on arterial stiffness associated with accelerated senescence in SAMP1 mice.